A Comparison of the Transverse, Axial and Radial Flux PM Synchronous Motors for Electric Vehicle

Bo Zhang, Torsten Epskamp, Martin Doppelbauer
Faculty of Electrical Engineering
Karlsruhe Institute of Technology
Karlsruhe, Germany
bo.zhang@kit.edu

Matthias Gregor
RD/RPT
Daimler AG
Stuttgart, Germany

***Abstract*—This paper presents the performance comparison among three different topologies of the permanent magnet synchronous machine, namely a transverse flux permanent magnet machine with flux concentration and claw pole structure, an axial flux machine with segmented armature torus structure and a conventional radial flux machine with embedded permanent magnets in the rotor. With the help of Finite Element Method, three electrical machines have been designed considering the required dimensions and permanent magnets mass. The complete results evaluation and comparisons are described in this paper. From the obtained results it can be concluded, the axial flux machine with segmented armature torus structure can be a competitive alternative compared with the conventional radial flux machine for applications with limited axial length, while the transverse flux machine is an attractive alternative for the high torque and low-speed applications due to its high pole number.**

Keywords—axial flux motor, segmented armature torus structure, soft magnetic composites, transverse flux motor with claw poles, three-dimensional finite element method

I. INTRODUCTION

The progress in the field of material technology is of great importance for the development of electrical machine. For instance, the application of permanent magnets (PM) in the electrical machine, especially the rare earth PM with high energy density, has improved the efficiency, reliability and power density significantly. Another attractive material is the soft magnetic composites (SMC), which are produced from iron powder coated with an electrically insulating layer. Compared with the conventional electrical steel, the SMC has a lot of advantages such as magnetic and thermal isotropy, lower eddy current losses, easy and cost effective manufacturing process with good tolerance and surface quality [1]-[2]. Based on the outstanding benefits, the SMC exhibits great potential for application in electrical machines with complex flux path and structure [3].

The concept of transverse flux machine (TFM) was proposed by Weh and May in 1896. Different from the conventional longitudinal flux machine (LFM), the main flux flows within a path transverse to the direction of rotation in TFM, which makes the decoupling of electric and magnetic loading and high pole number possible [4]-[5]. In order to guide the magnetic flux three-dimensionally (3D) in the TFM, the SMC is used to produce the complex electromagnetic parts. In addition, it is easier to produce the TFM with many phases, because each phase of TFM is independent und there is no magnetic coupling between them. Because of these characteristics, the TFM is processes high torque density and efficiency. However, the disadvantages of TFM should also be taken into account. First of all, the complex structure of TFM with 3D magnetic fields results in great difficulties in the manufacturing and assembly. Besides, the power factor of TFM is low due to its large inductance [6].

Another potential application for the SMC is the axial flux permanent magnet machine (AFPM), whose air-gap flux is mainly axial. Similar to the TFM, the SMC is used in AFPM to conduct the 3D magnetic flux in the rotor yoke and stator. Due to the application of PM with high energy density and larger air-gap area, the torque density and efficiency are significantly improved. Moreover, because of its short axial length and compact construction the AFPM is suitable for some special applications where the space is limited [7]-[9].

Both AFPM and transverse flux permanent magnet machine (TFPM) have 3D magnetic flux paths and complex structures. In addition, the permeability and saturation flux density are lower than the laminated steel. For these reasons, the selected TFPM and AFPM are modeled and analyzed using 3D finite element method (FEM), so that a very high accurate calculation of magnetic field distribution and motor characteristics can be implemented. For a better comparison, a radial flux machine with embedded PM in the inner rotor (RFPM) is designed due to the conventional type, which complies with same boundary conditions as TFPM and AFPM [10].

II. TOPOLOGIES DEFINITION OF ELECTRICAL MACHINES

First of all, the topologies of TFPM, AFPM and RFPM are researched and three of them are selected considering the torque density, efficiency and structure complexity. Based on the analytical calculation and accurate FEM, the three different machines are designed and optimized. For a better comparison, the number of phases, the dimensions and the mass of PM are maintained constant. In addition, the number of turns of the coils is so determined, that the current density in all motors are

PMG Füssen GmbH is the sponsor of SMC material for the prototyping.

978-1-4799-6075-0/14/$31.00 ©2014 IEEE

approximately the same.

A. *TFM with Claw Pole Structure*

During the past years, a large amount of work has been done to investigate the characteristics of TFM. Furthermore, a lot of structures have been developed to improve the torque density and to overcome the problem of complex structure. A notable improvement is the TFM with claw pole structure (CPTFM). By taking the magnetic decoupling of each phase and the periodical symmetry into account, only model of one pole pair, as shown in Fig. 1, needs to be investigated.

In order to realize the 3D conductivity of magnetic flux in the CPTFM, the stator with claw pole structure and the rotor are made from Somaloy700HR3P with relative high mechanical strength and permeability. The NdFeB permanent magnets with arc-shape are magnetized tangentially and embedded in the rotor. A toroidal winding is employed in each phase of CPTFM and enclosed by the stator core. The whole CPTFPM consists of three phases and there is a shifting of 120 electrical degrees among the phases.

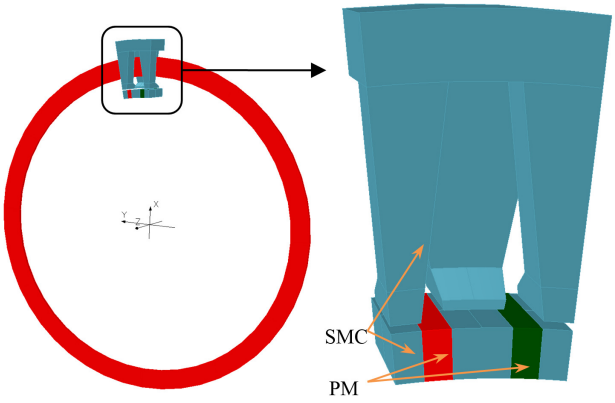

Fig. 1. Model of CPTFM in FEM

The main parameters of the designed CPTFM are listed in the Table 1.

TABLE I. MAIN PARAMETERS OF CPTFM

Symbol	Description	Value
D_a	Outer diameter	301 mm
D_i	Inner diameter	209 mm
L	Axial length of one phase	25 mm
p	Number of pole pairs	30
L_g	Radial length of air gap	1 mm
α_{PM}	Magnet pole-arc to pole pitch ratio	1/3
R_{PM}	Radial length of PM	6.4 mm
m_{PM}	Mass of PM	0.83 kg
w	Number of turns in the coil per phase	6

B. *Segmented Armature Torus Machine*

The AFPM is becoming attractive and used in more and more applications due to the high torque density, high efficiency and short axial length. The segmented armature torus machine (SAT) is a recent development of AFPM, as shown in Fig. 2. The SAT consists of two external rotors and an internal stator with a series of magnetically independent segments. Due to the application of rare earth PM with high energy density and the concentrated winding with short end-windings, the efficiency of SAT motor is significantly improved. In addition, the stator weight and iron loss are considerably reduced due to the absence of stator yoke.

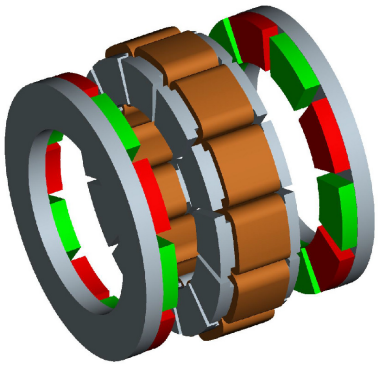

Fig. 2. Model of segmented armature torus machine

Similar to the CPTFM, the Somaloy700HR3P is used to produce the stator segments and the rotor yoke to conduct the 3D magnetic flux. The most important parameters of the designed SAT in this paper are listed in the Table 2.

TABLE II. MAIN PARAMETERS OF SAT

Symbol	Description	Value
D_a	Outer diameter	301 mm
D_i	Inner diameter	209 mm
L_{SAT}	Axial length of SAT	75 mm
p	Number of pole pairs	12
N_s	Number of stator segments	36
α_{PM}	Magnet pole-arc to pole pitch ratio	2/3
L_{PM}	Axial length of PM	2.2 mm
L_{yoke}	Axial length of rotor yoke	9.5 mm
m_{PM}	Mass of PM	0.83 kg
w	Number of turns per segment	22

Considering the periodic symmetry and the flux normal boundary condition along the xy-plane, only one twenty-fourth of the complete SAT is modeled and analyzed in FEM, as shown in Fig. 3. Different from the CPTFM, the PM with opposite magnetization direction are mounted on the surface of the rotor yoke.

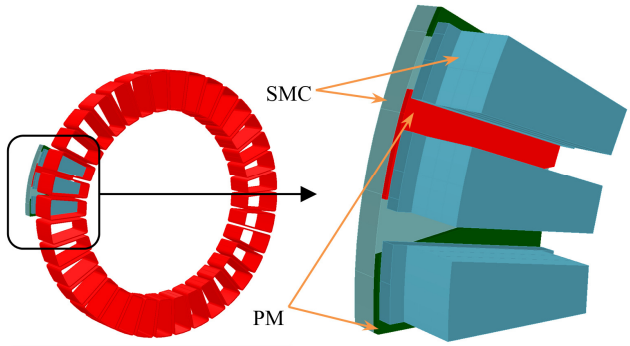

Fig. 3. Model of AFPM in FEM

C. *Conventional Radial Flux Machine*

To enable a better comparison, a widely used conventional radial flux permanent magnet machine (RFPM), as shown in Fig. 4, is designed, which consists of one external cylindrical stator and one cylindrical rotor with embedded PM. Similar to the SAT, a concentrated winding is used in the RFPM in order to achieve the required short axial length.

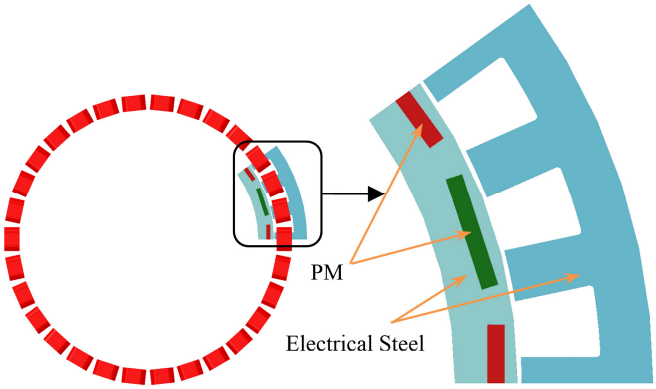

Fig. 4. Model of conventional RFPM in FEM

The main parameters of the RFPM are listed in Table 3. It should be noted that the dimensions, the mass of PM and the thickness of air-gap are the same as the CPTFM and SAT.

TABLE III. MAIN PARAMETERS OF RFPM

Symbol	Description	Value
D_a	Outer diameter	301 mm
D_i	Inner diameter	209 mm
L_{Core}	Axial length of iron core	49 mm
p	Number of pole pairs	10
N_s	Number of stator segments	30
R_g	Radial length of air gap	1 mm
L_{PM}	Axial length of PM per segment	7 mm
m_{PM}	Mass of PM	0.83 kg
w	Number of turns per coil	33

In order to reduce the torque ripple, the whole rotor consists of 7 segments and there is a rotation of 1 grad between the adjacent segments to reduce the torque ripple, as shown in Fig. 5.

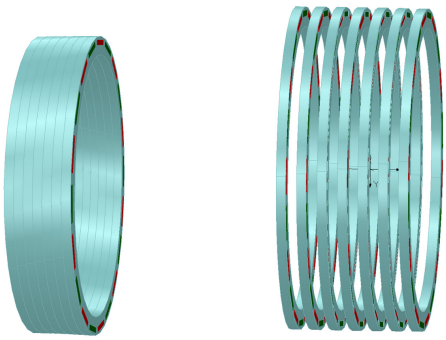

Fig. 5. Rotor of the RFPM

III. COMPARISON OF THE MOTORS

The various important characteristics of the three motors are evaluated and compared in details below. In order to achieve a high accuracy, the CPTFM and SAT are analyzed with the help of 3D FEM considering the existing 3D flux paths and complex structure. In comparison, the 2D FEM simulations have been performed for analysis of the conventional RFPM.

A. *Magnetic field and cogging torque with no-load*

The distribution of magnetic field and the flux density vectors within one pole-pair model of CPTFM, SAT and RFPM are investigated with the help of 3D FEA. For instance, the results under no-load condition are shown in Fig. 6.

For the CPTFM, It is evident that the flux produced from the two adjacent PM is concentrated in the SMC part of rotor and then flows to the air gap, which result in a high flux density and torque density. For this reason, it is noted that a high flux density at the tooth tip is reached. Finally, there is also a considerable amount of flux leakage between the side surfaces of the SMC parts in the rotor and claw poles.

Compared with CPTFM, the flux density in the stator teeth is lower in SAT. In order to reduce the torque ripple, the surface-mounted permanent magnets are skewed, which reduces the flux density in the stator segments as well as the average torque. For comparison, the results of RFPM with in a segment of the rotor are represented in Fig. 6. Similar to the CPTFM, the flux density in the RFPM is also very high, especially in the corner due to the leakage flux of PM. However, the saturation flux density of the electrical steel is much higher than SMC. As a result, the flux density is acceptable for RFPM and the over load capacity is better than the TFPM.

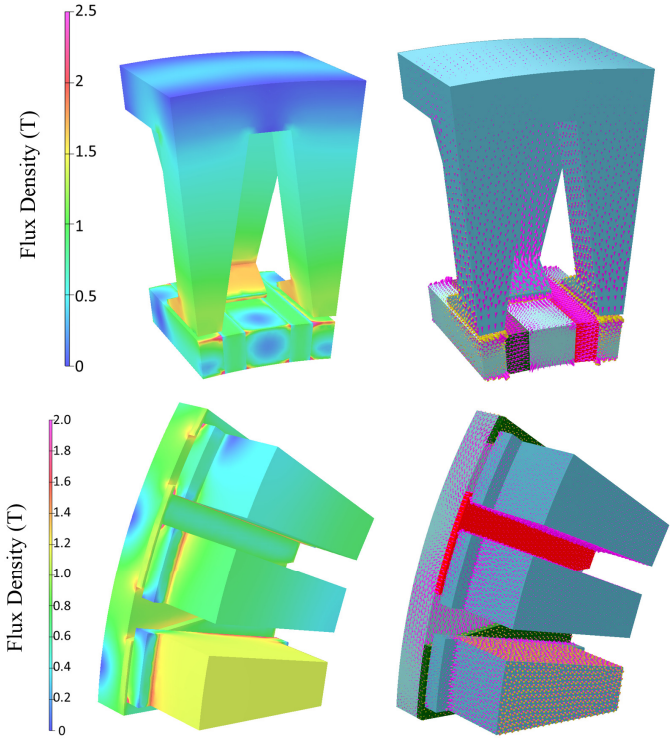

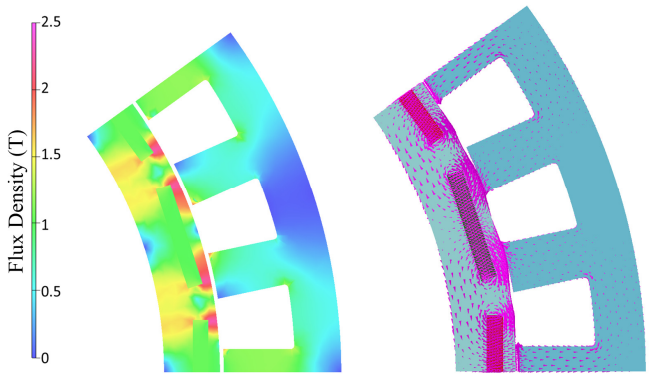

Fig. 6. Field distribution and flux density vectors of CPTFM (upper), SAT (middle) and RFPM (lower) with no-load

One of the main disadvantages of the permanent magnet synchronous machine with concentrated windings is the cogging torque, which is caused by the interaction of the magnet flux and stator teeth. It can raise the additional vibrations, acoustic noise and complicated starting conditions. Thus, the cogging torque of the machines is compared in Fig. 7.

It is noted that the RFPM possesses the lowest cogging torque due to the segmentation of the rotor, which can reduce the eddy current losses in the PM as well. Although the permanent magnets are skewed, the SAT has the highest torque ripple. This is because the topology with surface-mounted PM has generally a stronger interaction between the PM and the teeth and hence a higher cogging torque than the machines with embedded PM.

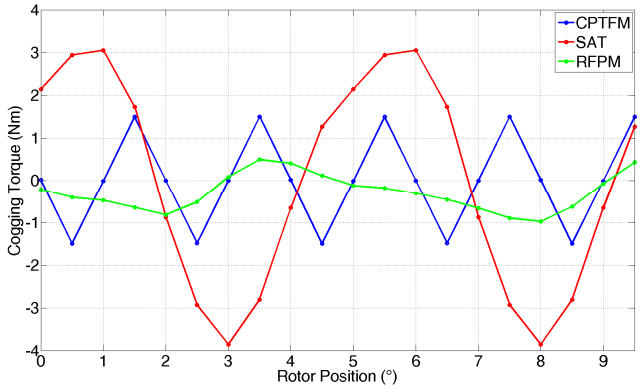

Fig. 7. Cogging Torque of CPTFM, SAT and RFPM

B. *Average Torque with different electrical Load*

The average torque under different electrical load is one of the most important issues to evaluate an electrical machine. The average torque of the three machines under different electrical load are compared in the Table 4 and Fig. 8.

It is noted that the CPTFM possesses the highest average torque when the electrical load is low. However, when the electrical load rises, the average torque of CPTFM becomes lower than the SAT, because the SMC in the CPTFM is more saturated than in the SAT. For the highest electrical load, which corresponds to an effective current density equals to 19.8 A/mm2, the average torque of CPTFM is already lower than that of the RFPM, where electrical steel with high saturation flux density are used. Because of the large air-gap area, the average torque of SAT is kept in a high level.

TABLE IV. AVERAGE TORQUE OF CPTFM, SAT AND RFPM

Peak Phase Current	CPTFM	SAT	RFPM
105 A	*77.8 Nm*	*53.2 Nm*	*43.9 Nm*
210 A	*144.2 Nm*	*106 Nm*	*88.1 Nm*
315 A	*194 Nm*	*157.6 Nm*	*131.8 Nm*
420 A	*226.9 Nm*	*207.7 Nm*	*173.6 Nm*
525 A	*244.5 Nm*	*255.1 Nm*	*212.6 Nm*
630 A	*260.9 Nm*	*296.2 Nm*	*247.8 Nm*
735 A	*273 Nm*	*334 Nm*	*278.6 Nm*
840 A	*282.2 Nm*	*367.7 Nm*	*305 Nm*

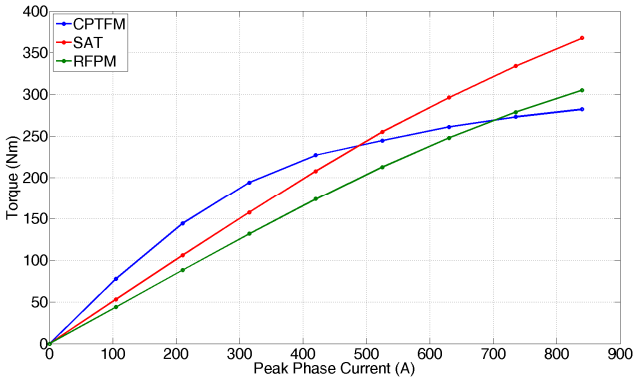

Fig. 8. Average Torque of CPTFM, SAT and RFPM

C. *Speed-Torque-Curve and Speed-Power-Torque*

The speed-torque-curves of the three electrical machines are calculated for the same specified inverter, whose maximum line voltage U_{rms} is equal to 167 and the maximum line current I_{rms} is equal to 300 A corresponding to a peak current density of 14 A/mm^2. The Fig. 9 shows the speed-torque-curves of the three different machines. In order to maintain the same current density, the machines have the specified number of turns of coil in the Table 1, 2 and 3. It is evident that for the peak current density equals to 14 A/mm^2 the CPTFM has the highest torque in the low speed area. However, when the maximum line voltage is achieved, the torque of CPTFM reduces significantly as the speed further increases.

In terms of the speed-torque-curve, the SAT exhibits the best characteristic for the specified electrical loading. Although the maximum torque is a bit lower than the CPTFM, the maximum torque maintains until the rotational speed is more than 3000. In the field weakening area, the torque of SAT is always higher than the RFPM. It should be noted that the comparison is carried out with the constant peak current density equals to 14 A/mm2. The results could be different for another electrical load.

Compared with the CPTFM and SAT, the RFPM possesses the lowest maximum torque at the low speed. However, the maximum torque can be maintained until the high speed equals to 3800 rpm.

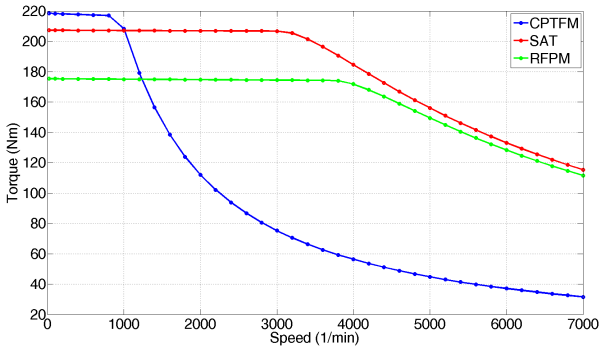

Fig. 9. Speed-Torque-Curve of CPTFM, SAT and RFPM with constant J

The corresponding speed-power-curves of the three machines are shown in the Fig. 10. It can be observed that the maximum output power of the CPTFM is much lower than the other two machines. This is because in CPTFM the number of pole pair is so large that the injected stator current is kept very low to reduce the line voltage and to achieve the required high speed.

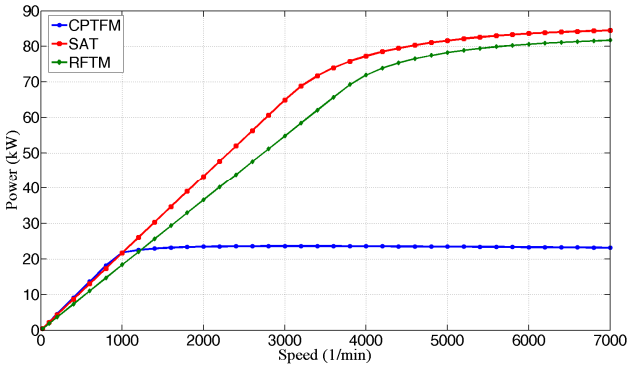

Fig. 10. Speed-Power-Curve of CPTFM, SAT and RFPM with constant J

The speed-torque-curve is closely associated with the number of turns of the coils. For a better comparison, it varies continuously so that a maximum torque equal to 200 Nm for all the machines is achieved. The results are presented in the Fig. 11. It is much clearer that the SAT possesses the highest speed when the maximum line voltage is achieved. Meanwhile the SAT exhibits the highest torque in the field weakening area.

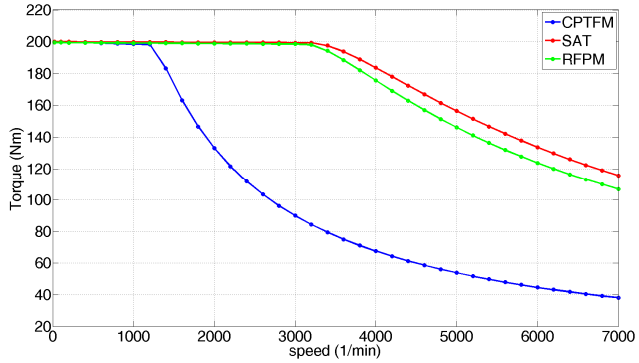

Fig. 11. Speed-Torque-Curves of CPTFM, SAT and RFPM with constant maximum Torque

D. *Comparison of Efficiency Map*

With the help of the informative efficiency map, the characteristics of an electrical machine can be well evaluated. The corresponding efficiency maps of the three machines, which have a varied number of turns in coils to achieve the same maximum torque, are evaluated and compared in Fig. 12.

It is noted that the efficiency of all three machines are very excellent due to the application of rare earth permanent magnets and windings with high fill factor. In summary, the SAT has the highest efficiency and the largest area with high efficiency. Compared with SAT and RFPM, the CPTFM exhibits a high efficiency over a wide speed range, especially in the area with low torque at low speed.

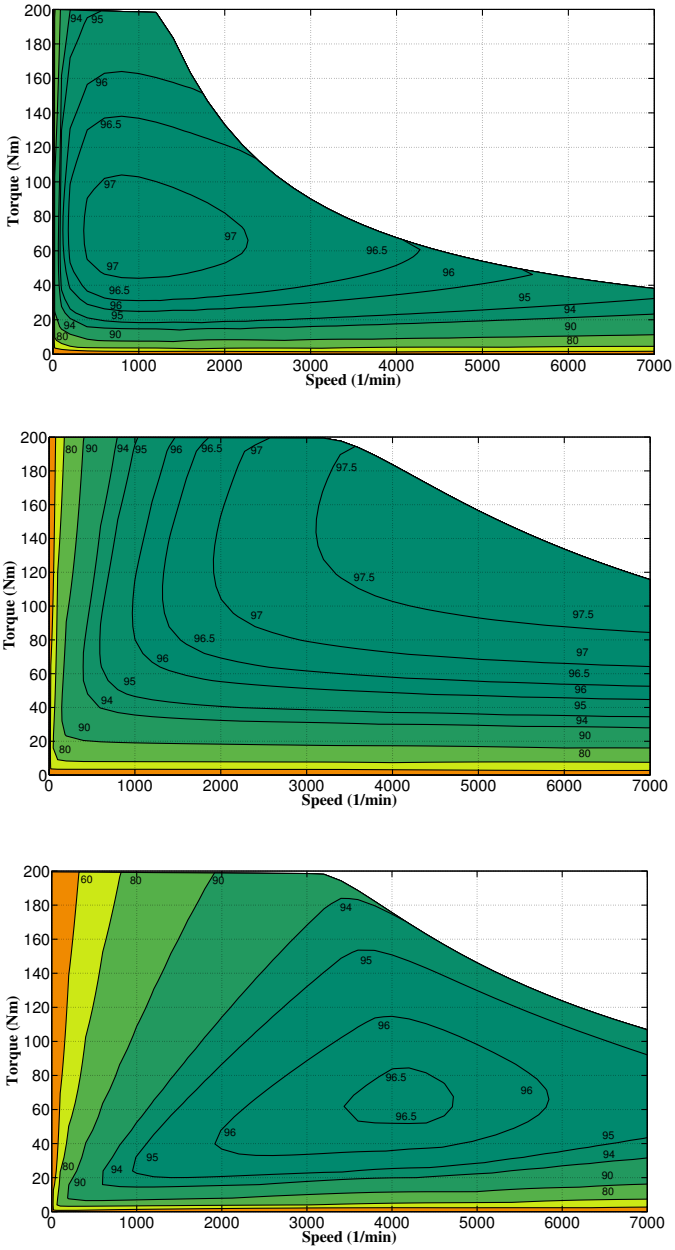

Fig. 12. Efficiency Maps of CPTFM (upper), SAT (middle) and RFPM (lower)

Bases on the above research, it is obvious that the CPTFM is suitable for the applications when low speed, high torque and low electrical load are required. When the axial length is limited, the SAT becomes a more competitive alternative to the conventional RFPM.

IV. CONCLUSION

In this paper, with the help of FEM a transverse flux machine with flux concentrating and claw pole structure (CPTFM), an axial flux segmented armature torus machine (SAT) and a conventional radial flux machine with embedded permanent magnets (RFPM) are designed, evaluated and compared, which have the same dimensions and identical PM mass. For a better comparison, the number of the turns in the coil of the machines is so determined, that the same current density is achieved. It is concluded that for the low electrical load, the CPTFM has the highest torque. However, the SMC in CPTFM can be more easily saturated leading to a poor over load capacity. In comparison, the SAT exhibits a higher torque than the CPTFM and RFPM for high electrical load.

The speed-torque-curves and the efficiency maps of the three machines are calculated for the specified inverter. It is noted that the torque of the CPTFM reduces dramatically in the field weakening area because of the high induced voltage caused by the high pole number, while the SAT exhibits a high torque over a wide speed range and a large area with high efficiency. In conclusion, the CPTFM is suitable for the application when low speed and high torque are required and the electrical load is low. When the axial length is limited, the SAT becomes an interesting alternative to the conventional RFPM.

REFERENCES

[1] A. Boehm, and I. Hanh, "Comparison of soft magnetic composites (SMCs) and electrical steel," presented at the 2nd Int. Conf. Electric Drives Production Conference (EDPC), Nuremberg, Germany, 2012.

[2] L. O. Hultman and A. G. Jack, "Soft magnetic composites-materials and applications," in *2003 IEEE Electric Machines and Drives Conf. (IEMDC'03),* pp. 516-522.

[3] J. G. Zhu and Y. G. Guo, , " Study with magnetic property measurement of soft magnetic composite material and its application in electrical machines," in *IEEE 2004 Industry Applications Conference, 39th IAS Annual Meeting*.

[4] E. Schmidt, "Finite Element Analysis of a Novel Design of a Three Phase Transverse Flux Machine with an External Rotor," *IEEE Trans. On Magnetics*, 2011, pp. 982-985.

[5] D. J. Bang, H. Polinder, G. Shrestha, and J. A. Ferreira, "Design of a lightweight transverse flux permanent magnet machine for direct-drive wind turbines," in *Proc*. 2008 *Industry Appl. Soc. Annu. Meeting,* pp. 1–7.

[6] J. G. Zhu, Y. G. Guo, Z. W. Lin, and Y. J. Lin, "Development of PM Transverse Flux Motors With Soft Magnetic Composite Cores," *IEEE Trans. On Magnetics*, 2011, pp. 4376-4383.

[7] M. Aydin, S. Huang and T. A. Lipo. "Axial Flux Permanent Magnet Disc Machines: A Review," Conf. Record of SPEEDAM, pp. 61-71, 1994.

[8] T. J. Woolmer, and M. D. McCulloch. "Analysis of the Yokeless and Segmented Armature Machine," *IEEE International Electric Machines & Drives Conference*, pp. 704-708, 2007.

[9] W. Fei, P. Luk, and K. Jinupun, "A new axial flux permanent magnet Segmented-Armature-Torus machine for in-wheel direct drive applications," *IEEE Power Electronics Specialists Conf., 2008*, pp. 2197-2202.

[10] A. Cavagnino, M. Lazzari, F. Profumo, and A. Tenconi, "A comparison between the axial flux and the radial flux structures for PM synchronous motors," *IEEE Transactions on Industry Applications,* Dez. *2002,* pp. 1517-1524.